

Adaptive Rectifier Driven by Power Intake Predictors for Wind Energy Harvesting Sensor Networks

Danilo Porcarelli, Dora Spenza, Davide Brunelli, Alessandro Cammarano, Chiara Petrioli, and Luca Benini

Abstract—This paper presents a power management technique for improving the efficiency of harvesting energy from air-flows in wireless sensor networks (WSNs) applications. The proposed architecture consists of a two-stage energy conversion circuit: an AC-DC converter followed by a DC-DC buck-boost regulator with Maximum Power Point Tracking (MPPT) capability. The key feature of the proposed solution is the adaptive hybrid voltage rectifier which exploits both passive and active topologies combined with power prediction algorithms. The adaptive converter significantly outperforms other solutions, increasing the efficiency between 10% and 30% with respect to the only-passive and the only-active topologies. To assess the performance of this approach in a real-life scenario, air-flow data have been collected by deploying WSN nodes interfaced with a wind micro-turbine in an underground tunnel of the *Metro B1* line in Rome. It is shown that, by using the adaptive AC-DC converter combined with power prediction algorithms, nodes deployed in the tunnel can harvest up to 22% more energy with respect to previous methods. Finally, it is shown that using power management techniques optimized for the specific scenario, the overall system overhead, in terms of average number of sampling performed per day by a node, is reduced of up to 93%.

Keywords—Energy harvesting, power management technique, prediction algorithm, voltage rectifier, wireless sensor networks.

I. INTRODUCTION

RESEARCH in power aware systems has gained increasing interest in recent years, pushing the exploration of new ultra low-power and energy autonomous hardware architectures and the investigation of new algorithms for power generation, estimation, profiling, prediction and management. In particular, significant attention has been devoted to emerging energy harvesting technologies, which allow to power embedded distributed systems, such as wireless sensor networks, indefinitely in time by scavenging energy from the environment [1]–[3].

Danilo Porcarelli is with the University of Bologna, Bologna, Italy (e-mail: danilo.porcarelli@unibo.it).

Dora Spenza, Alessandro Cammarano and Chiara Petrioli are with the “Sapienza” University of Rome, Rome, Italy (e-mail: {surname}@di.uniroma1.it).

Davide Brunelli is with the University of Trento, Italy (email: davide.brunelli@unitn.it).

Luca Benini is with the University of Bologna, Bologna, Italy and with ETH Zurich, Switzerland (e-mail: luca.benini@unibo.it).

The research contribution presented in this paper has been supported by project GENESI - GrEen sensor NEtworks for Structural monitoring (grant n.257916) and by project GreenDataNet (grant n.609000) both funded by the EU 7th Framework Programme.

In addition, Dora Spenza gratefully acknowledges support from the 2010 Google Europe Doctoral Fellowship in Wireless Networking.

Finally, the authors would like to thank ROMA METROPOLITANE s.p.a. for the unique and exclusive site offered for the deployment.

Many works have explored energy scavenging opportunities in different application scenarios, focusing, for example, on architectures for harvesting energy from vibrations [4], electromagnetic fields [5] or heat [6], which can provide power densities in the microwatt range. Solar light, however, remains the most investigated energy source [7]–[9], thanks to the fact that even small solar cells are able to deliver power densities in the milliwatt range. Another very attractive source providing energy in the milliwatt range is air-flow. For example, the small micro-wind turbine used in [10] and [11] with a diameter of just 6.3cm can generate power in the range 10 – 100mW.

The architecture of air-flow energy harvesters typically exhibits an initial rectifier stage to convert the AC output of the turbine into a more suitable DC signal, and a second regulation stage to perform MPPT, store the energy and supply the user system [11]–[13]. Typically, the rectifier circuits used in ultra-low power applications are divided into two categories, namely *passive* and *active*.

Passive rectifiers, which are usually realized through a diode full wave bridge, are the simplest and commonly used topologies. However, they are also the least efficient, due to the high voltage drop across the diodes during the forward polarization (about 0.6V – 0.7V using common Silicon Diffused Junction diodes, 0.2V – 0.3V using Schottky diodes).

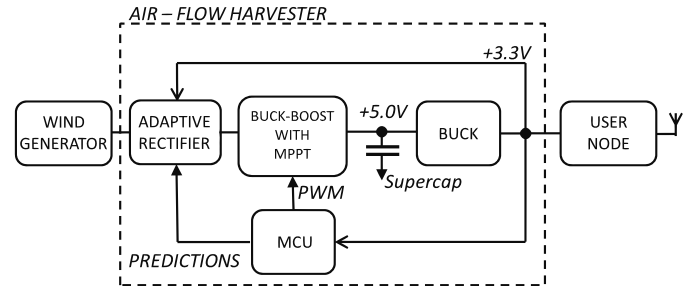


Fig. 1. Block diagram of the proposed air-flow energy harvester

Active rectifiers improve the conversion efficiency by replacing diodes with MOSFETs, which significantly reduce the voltage drop in the ON-state. Such additional efficiency, however, increases the complexity and the cost of the system, due to the presence of control circuitry for the MOSFETs. When the micro-wind turbine generates low rectified voltage levels (e.g., $V_C < 1.8V$), such that the control circuit is switched off, the conversion is performed by the parasitic diodes of the transistors. This means that there is a transition threshold between the passive and the active operating modes, and therefore between a lower and a higher efficiency AC-DC conversion. The *active* rectifier optimizes the efficiency

when the wind speed generates an input power greater than the transition threshold, but whenever the incoming power falls below the transition threshold the conversion efficiency is the same as a classical full-wave bridge. In this latter case, a Schottky rectifier would perform much better.

The goal of the presented work is the design of a hardware and software power management technique to improve the efficiency of the rectifier stage. Power management solutions for environmentally-powered systems have to deal with the variable nature of ambient power sources, which results in significant fluctuations in the amounts of energy over time. To mitigate this shortcoming, energy prediction methods are employed to forecast the availability of the power source and to estimate the expected energy intake generated by air-flows in the near future. Such predictors allow the system to take critical decisions about the utilization of the available energy, enabling the development of *pro-active* power management strategies.

The block diagram of the system discussed in this work is shown in Fig. 1. It features a hybrid adaptive rectifier stage that exploits both the *active* and *Schottky-passive* topologies to achieve the maximum efficiency over the whole range of air-flow speed. In addition, an efficient power management stage, controlled by an ultra-low power micro-controller, converts and stores the incoming energy. The micro-controller elaborates periodically the prediction of the power intake from air-flow data, delivers estimations about the energy availability in the near future, and determines which topology of rectifier is the most efficient under certain air-flow speed conditions. To show the benefits of the adaptive AC-DC converter in a real-life scenario, the practical case of a WSN deployed in an underground tunnel is considered, where nodes are able to harvest energy from air-flows. More in detail, real-life air-flow data have been collected for 33 days by instrumenting a tunnel of the *Metro B1* line in Rome, Italy, with Telos B motes equipped with wind micro-turbines [14]. Then, the usable power obtained from passing trains is estimated for each rectifier by considering the efficiency values previously calculated. In such scenario, the average energy harvested per day by using the adaptive converter is up to 18% higher than that harvested by the passive-Schottky-only topology and up to 22% higher than that harvested by the active-only topology.

The underground tunnel environment is almost totally predictable, as underground trains generally transit with a regular schedule and with approximately the same speed. By exploiting such regularity, a power management technique that is specifically tailored to the underground tunnel scenario is devised. It allows to reduce the overall overhead of the system, rated as the average number of sampling performed per day by a node using a given power management policy, of up to 93%, without impairing the energy harvesting process.

The rest of the paper is organized as follow: Section II gives an overview of the state of the art on the architecture of air-flow harvesters, rectifiers design and power management and prediction algorithms. Section III presents a detailed description of the hybrid system and the energy harvester adopted. Section IV is dedicated to the analysis of air-flow data collected during tunnel monitoring, while Section V discusses the power management algorithms. Finally, results are dis-

cussed in Section VI, followed by conclusions in Section VII.

II. RELATED WORKS

Deployments of WSNs in tunnels have been described and discussed in previous works [15]–[21]. Colesanti *et al.* describe in [15] their on-the-field experience with a battery-powered Wireless Sensor Network deployed on a construction site of the Rome B1 underground for structural health monitoring. In [16], Ceriotti *et al.* report on a deployment in which a WSN is a key component of a control system for adaptive lighting in road tunnels. In [17], Mottola *et al.* present two WSN deployments in an operational road tunnel and in a nonoperational one. They compare the wireless topology in the two scenarios, in terms of reliability, stability, and asymmetry of links, providing results about the impact of such topologies on MAC and routing layers. In [18], Stajano *et al.* discuss their experience with a WSN testbed composed of 26 nodes deployed in a London Underground tunnel on the Jubilee Line to measure changes in displacement, inclination, temperature and relative humidity. In [19] the development and deployment of a WSN to monitor a train tunnel during adjacent construction activity is described. The majority of such works focused on connectivity issues in tunnel scenarios and none reported the deployment of WSN nodes with energy harvesting capabilities in underground tunnels. Energy-harvesting WSNs exhibit unique characteristics and one of the key aspects they have to cope with, is the significant fluctuations in the energy availability over time. To mitigate such aspect, several energy prediction models have been proposed recently by the research community, with the goal of providing energy forecasting for real-time systems [22], [23] and over short and medium timeframes [24]–[30].

One of the first prototypes of air-flow harvesters was developed with the aim of extending the lifetime of a WSN for wind speed sensing [13]. The same anemometer used to perform measurement is connected to a small alternator to harvest energy, while a buck-boost converter operated in DCM provides the regulated voltage to recharge a battery with a maximum efficiency of 72%. Furthermore, the power transfer is optimized by biasing the alternator, maintaining constant the input resistance of the converter. As the AC-DC converter is formed by a Schottky full-wave rectifier, the overall efficiency of the architecture should be in the range 50% – 55%. The resistance emulation approach to perform MPPT in energy harvesting systems is well known from power electronics for big wind turbine systems [31], [32] and discussed in depth for low power systems by Paing *et al.* in [33]. They proposed a theoretical method to estimate the power consumption of the most common topologies of DC-DC converter as a function of critical parameters such as switching frequency and duty cycle, concluding their work with an example of buck-boost converter suitable for wind harvesting. Such technique was later elaborated and exploited in several recent works, such as [12], [34], where the authors modeled and characterized a micro-wind turbine with a sinusoidal output signal and a diameter of 6cm. The AC signal is rectified by a full-wave Schottky bridge and the design method of a buck-boost converter optimized

to achieve a high conversion efficiency is presented. The converter efficiency of 81%–87% combined with the Schottky bridge leads to an overall efficiency between 50% – 65%. A similar wind generator is used in [11] for delivering energy to a self-powered node. The conversion circuit consists of an active full wave rectifier followed by a boost converter with resistance emulation capability combined with a micro-controller to perform MPPT. The active rectifier, realized with off-the-shelf components, increases the efficiency up to 70% when compared to a Silicon Diffused Junction diode-passive rectifier with a low input voltage of 1.2V, reaching peak values of about 80%. Thus, considering the high conversion efficiency of the regulation stage (80% – 90%) the overall architecture performs with an efficiency greater than 70%. Nevertheless, this solution exploits the bulk parasitic diodes of the MOSFETs as alternative way to perform rectification when the control circuit cannot work, resulting in a significant loss of overall efficiency (lower than 50%).

The design of an efficient rectifier is challenging in energy harvesting applications, especially when dealing with microwatt sources. Several works presented in literature are based on the principle of replacing the passive elements (the diodes) with active ones, usually called active diodes as they work as diodes but need control circuitry. Moreover, to achieve higher efficiency the majority of researchers have investigated only integrated solutions. For example, the circuit proposed in [35] exploits linear-region operated MOSFETs to emulate diodes and the control circuitry is directly powered from the input signal. Such system, simulated and realized in 130nm technology can extract up to 90% of the maximum power from an ideal piezoelectric device. In [36] an integrated bridge fabricated in 0.35 μ m CMOS process is described, in which the four diodes are replaced by two cross-coupled P-channel MOSFET transistors and two active diodes driven by two 4-input comparators. Such configuration matches a zero-threshold diode and effectively eliminates the reverse current increasing the overall efficiency up to 90%.

Another widely explored method to design rectifier is the voltage multiplying technique. The active voltage doubler presented in [37], realized in 5V CMOS STMicroelectronics technology, uses two switching MOSFETs driven by operational amplifiers instead of comparators and shows an efficiency between 75% and 95%. Finally, Cheng *et al.* propose an active voltage doubler [38] and an 8 \times active voltage multiplier [39] exploiting active diodes technique and using off-the-shelf components. The voltage doubler can reach more than 80% efficiency for input voltage amplitudes greater than 0.25V while the 8 \times multiplier can recharge a 3.7V lithium battery with over 80% efficiency.

All the mentioned active rectifiers are optimized to work in piezoelectric or RF harvesting applications and are designed to maximize the efficiency with very low input voltage and power because it is crucial to avoid power wasting in the *microwatts*. Complex systems, featuring a very low start-up voltage and high conversion efficiency are fundamental in these conditions. The hybrid solution presented in this paper is realized with off-the-shelf components and represents a cost effective design suitable for environmental sources which

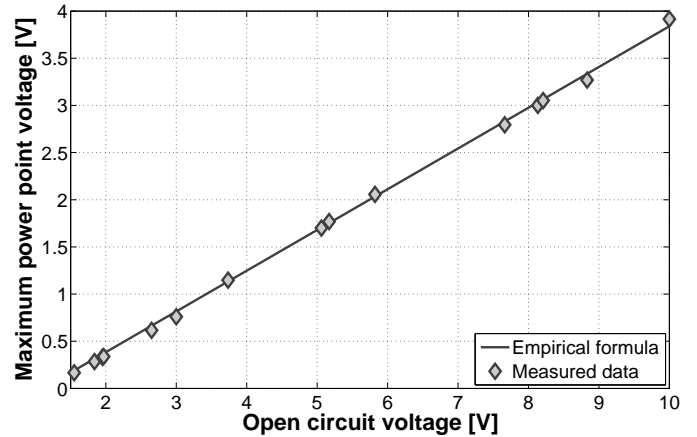


Fig. 2. Relation between open circuit voltage and maximum power point voltage of the micro-turbine. The solid line represents the empirical formula while the dots the measured data.

produce *milliwatts*, as the air-flow energy harvesting. In these conditions, the proposed solution is simpler and achieves performance comparable to the on-chip rectifiers.

III. ARCHITECTURE OF THE ENERGY HARVESTER

The adaptive rectifier presented in this paper was originally designed to improve the efficiency of the air-flow path of the multi-source energy harvester discussed in [10]. This air-flow harvester consists of a two-stage architecture, more precisely a passive-Schottky-diode full-wave rectifier followed by a buck-boost converter which recharges a supercapacitor used as a local energy buffer. In this work the passive rectifier is replaced with an adaptive one. As shown in Fig. 1 an ultra low-power MCU performs power management, namely it selects the optimal rectifier and performs the MPPT algorithm to maximize the conversion efficiency. Finally, an output buck converter provides the regulated power supply to the micro-controller and to the supplied platform.

A. Wind Generator

The air-flow transducer used in this work is a small plastic four-bladed horizontal axis micro-wind turbine, which produces a sinusoidal power signal, whose amplitude and frequency is dependent on the air speed. The maximum power transfer is reached when a load in the range 500 – 700 Ω is applied. Experiments show that the optimal load value is 560 Ω . An exhaustive characterization of this micro-turbine with simulations and experimental results is given in [12]. In addition, some experiments were conducted to derive the following empirical formula:

$$V_{MPP} = V_{OC} \times K_{MPP} - \alpha_{MPP} \quad (1)$$

that shows the relation between the open circuit voltage (V_{OC}) and the maximum power point voltage (V_{MPP}) of the micro-turbine. More precisely, during the characterization process of different micro-turbines a quasi-linear relation between the measured values of the open circuit voltage and the MPP voltage has been noticed. Thus, the linear equation 1 is used

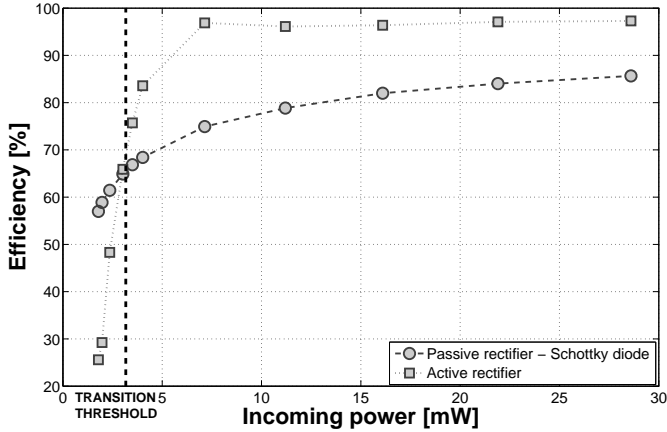


Fig. 4. Efficiency comparison of the simulated passive-Schottky and active rectifiers. The efficiency is calculated at the optimal load resistance of 560Ω . The vertical dashed line shows the efficiency transition threshold.

to calculate the MPP voltage exploiting the measured open circuit values. Both K_{MPP} and α_{MPP} depend on micro-turbine physical parameters such as diameter or number of turns. The adopted micro-turbine features $K_{MPP} = 0.4319$ and $\alpha_{MPP} = 0.48V$. Equation 1 will be used during data analysis discussed in Section IV. In Fig. 2, the measured data compared with the empirical formula are proposed.

B. Hybrid Full-Wave Rectifier

The schematic, in Fig. 3, shows in detail the design of the adaptive rectifier, as a sub-circuit of the whole harvester. The passive stage is a full-wave bridge implemented with four Schottky diodes ($D1 - D4$), while the active stage uses P-channel MOSFETs $M1 - M2$ and N-channel MOSFETs $M3 - M4$ as rectifying elements. The control circuit exploits two fast-switching ultra low-power comparators $U1 - U2$. During the positive half-wave $M1$ and $M3$ are switched-ON, forming a conductive path to the filter capacitor $C1$ and ground, respectively, while $M2 - M4$ are switched-OFF. Vice-versa $M2 - M4$ are in conduction during the negative half-wave and $M1 - M3$ are OFF.

$C1$ is a small smooth capacitor of $220\mu F$ used to limit the ripple of the input power and also to provide a suitable voltage supply V_C to the ultra-low power comparators $U1$ and $U2$. The control circuit, powered by the capacitor $C1$, continuously monitors the AC source current by means of the sensing resistors $R1 - R2$. Comparators $U1 - U2$ are used to generate the proper gating signals for $M1 - M4$. A thorough discussion about the benefits of this current-sensing approach is given by Tan *et al.* in [11].

The performance of both rectifiers is evaluated individually by means of SPICE simulations which took into account the power drawn by the control circuit of the active and adaptive topologies. The characterization process was conducted by using a variable resistor as a load. The results are plotted in Fig. 4, which compares the efficiency of the active and passive-Schottky rectifiers. The Schottky diodes, with their $0.2 - 0.3V$



Fig. 5. Snapshot of nodes deployed in a tunnel of the Metro B1 line in Rome.

voltage drop in conduction mode, are a very attractive solution in case of low power intake. As shown in Fig. 4, there is a transition threshold which delimits two operating areas: with an input power in the range $0 - 2mW$ the Schottky rectifier (dashed line marked with circles) performs conversion with an efficiency of $60\% - 70\%$, outperforming the active rectifier (dotted line marked with squares) by $10 - 40\%$. Conversely, when the power intake exceeds the threshold of $2mW$ the active rectifier is the most efficient topology to use with a peak of 96% of efficiency.

Thus, for each operating region there is an optimal solution. When the input power is below the transition threshold the Schottky rectifier is preferable, while the active topology is much better with input power above the threshold. The design allows to dynamically select the most suitable topology by means of the selector circuit, thus power management policies will adjust adaptively to the optimal configuration as described in detail in Section V.

The selector consists of a small latching-coil relay driven by a MOSFET H-bridge, not shown in the figure for the sake of simplification. The relay is a bistable device which features two SPDT switches. Each stable state can be reached by energizing the coil with a short pulse of current of $5ms$. The mechanical contacts reduce the voltage drops across the switches and a single commutation needs only $340\mu J$ of energy. In our case, the wind conditions will be evaluated every $10s$, and thus the relay will be switched every $10s$, at worst. The average power calculated in this interval is therefore less than $34\mu W$.

C. MPPT Circuit and Output Stage

To achieve maximum power transfer the conversion circuit has been designed to emulate the equivalent input resistance discussed in Section III-A. The present work exploits the buck-boost converter depicted in Fig. 3 (*CONVERSION STAGE*), implemented with off-the-shelf components and operated in Fixed Frequency-Discontinuous Current Mode (FF-DCM) to emulate the optimal input impedance value of 560Ω and stores the converted energy in a $1F, 5.5V$ supercapacitor. The PWM gating signal is generated by an ultra low-power micro-controller according to the formula:

$$R_{IN,eq} = \frac{2L}{d^2T} \quad (2)$$

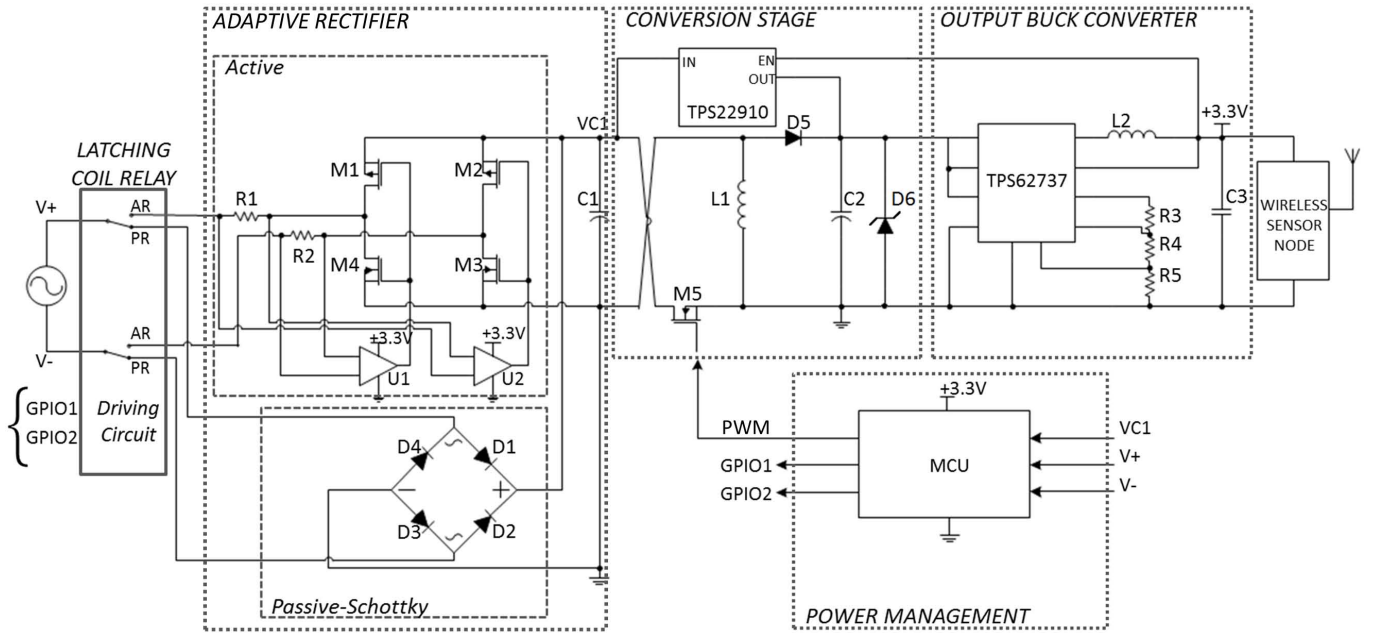


Fig. 3. Schematic of the complete air-flow energy harvester including the hardware implementation of the adaptive rectifier, the selector circuit, the buck-boost-based conversion stage and the output DC-DC stage.

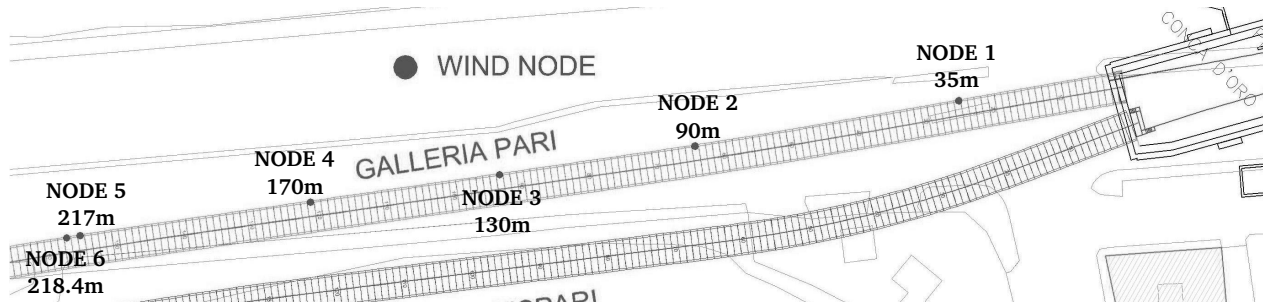


Fig. 6. Position of the nodes deployed in the tunnel and their distances from the train station. (Site plan courtesy of Roma Metropolitana and Tre Esse Engineering, FP7 GENESI project).

where L is the value of the inductor $L1$, T and d are the period and the duty cycle of the PWM signal respectively. In equation (2) the input equivalent resistance is the only constraint to satisfy, thus the remaining three degrees of freedom are used to size the inductor value, the frequency and the duty cycle by solving a system of equations which minimizes the converter losses [12]. This converter performs with an overall efficiency of 85%, starting from the minimum value of 83% and rising over 86% when the input power is greater than $6mW$.

The output stage in Fig. 3 (*OUTPUT BUCK CONVERTER*) consists of the integrated buck converter TPS62737 from Texas Instruments. It provides a regulated 3.3V supply for the relay, the micro-controller and the powered system consuming only $380nA$ of quiescent current when active. The cold boot of the system is guaranteed by the active-low TPS22910 load switch from Texas Instruments. In worst case conditions, namely when the supercapacitor is empty and it is not possible to

perform any MPPT algorithm, the rectification is performed by the Schottky bridge, while the supercapacitor is recharged exploiting the alternative path provided by the switch, which bypasses the buck-boost converter and directly connects the rectifier to the supercapacitor. When the voltage across the supercap rises up to the minimum operating voltage of the TPS62737 (i.e., the converter output reaches the value of 3.3V suitable to supply the micro-controller and the adaptive rectifier) the switch is opened and the supercapacitor is efficiently recharged exploiting the buck-boost converter performing the MPPT algorithm. Finally, to avoid damages due over-voltage conditions, the supercapacitor is protected by means of the zener diode D6.

IV. REAL-LIFE AIR-FLOW DATA COLLECTION

This section is dedicated to the analysis of the air-flow conditions of the underground tunnel used as test scenario. The data collection was performed in a tunnel of the new

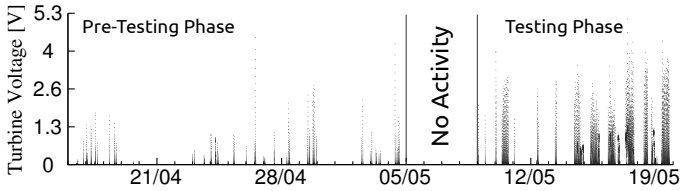


Fig. 7. Turbine open circuit voltage detected during the three phases of the train test in the tunnel on the Metro B1 line. Data are those collected by the node with *id* 1.

Underground *Metro B1* line in Rome and took place after the construction phase of the tunnel was completed. More specifically, air-flow data were recorded in the pre-testing and testing phases of the new tunnel during which trains, as well as other vehicles used in construction works, were operated for testing purposes. Six Telos B motes [40] equipped with a wind micro-turbine followed by a Schottky bridge were used to instrument 220m of tunnel with the aim to collect air-flow data generated by passing trains (and vehicles) for 33 days. Figure 6 shows the nodes deployment in the tunnel and their distance from the *Conca D'Oro* train station. A dedicated TinyOS [41] application has been developed to track the voltage of the filter capacitor every 2s. Whenever the measured voltage was higher than 3mV, the collected data was stored in the node flash memory and marked with a time-stamp corresponding to the local time of the node. These voltage values were converted to the respective maximum power point voltage values in post-processing by using Equation (1).

The nodes deployed in the tunnel of the *Metro B1* line were placed all at the same height along one side of the tunnel. The distance between consecutive nodes was variable, to allow to test air-flow data correlation in different conditions. Figure 5 shows a snapshot of two deployed nodes.

A. Collected Air-flow Data

Nodes were deployed in an Underground tunnel of the Metro B1 line in Rome for 33 days, from April 16th, 2012 to May 19th, 2012.

Fig. 7 shows the three distinct phases of the Metro B1 train test during the period in which data were collected:

- (i) A pre-testing phase, in which most of the detected events were related to the movement of vehicles used in construction work.
- (ii) A phase of no activity, during which no passage in the tunnel was detected.
- (iii) A testing phase in which passing trains were detected.

Fig. 8 shows an example of data collected over one day by node 6, highlighting how harvesting events occurred fairly regularly.

B. Trains Passage Detection

The detection of train passage events has been performed by considering the changes in the measured voltage of the micro-turbines over time. More in details, the detection algorithm works as follows:

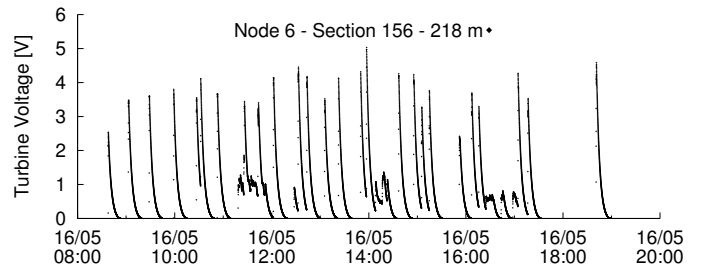


Fig. 8. Data collected by node 6 on the 16th of May 2012.

- 1) Whenever the voltage generated by the micro-turbine starts increasing, a potential event is detected and its start time t_s is annotated;
- 2) The end time of the event is the instant of time t_e after which the voltage generated by the turbine starts decreasing and keeps dropping for at least 30 seconds¹;
- 3) The energy generated in the period $[t_s; t_e]$ is computed as explained in Section IV-C. If the total energy intake in such period is below a minimum detection threshold, the event is discarded, as it is likely not related to a train passage, but rather to wind blowing in the tunnel.

Fig. 9 shows an example of detection of train passage events. The measured turbine voltage is shown in the y-axis, while in the x-axis time is reported. Dashed lines mark the time interval in which the event has occurred. As shows in the figure, three train passage events were detected, with an average train inter-arrival time of 12 – 30min. Table I reports the complete statistics about all the train passage events detected during the period 14 – 18 May 2012 by the six nodes deployed in the tunnel. More in details, the table shows, for each node, the total number of train passages detected, the mean inter-arrival time (MIT) and the standard deviation between the passage of two consecutive trains at daytime, and the average duration and standard deviation of each recharging event.

Such statistics are important because they are used by the nodes to estimate when the future energy recharging event is going to occur and for how long it is expected to last, thus allowing to devise pro-active strategies to plan in advance the energy usage. As reported in the table, results are quite similar for different nodes. Node 1 detects an average inter-arrival time lower than the other nodes. This is due to the fact that it is the node closest to the station, thus it is more exposed to air-flows that are not generated by trains passing in the tunnel. The average duration of its recharging events is also lower than that of other nodes, because trains decelerate when approaching the station.

C. Energy Intake Calculation

To calculate the energy intake generated by the micro-turbine during each train passage event, the open circuit voltage measured by the nodes has been converted to the

¹Such 30 seconds interval is used as guard time, because during train passage events the voltage of the turbine does not monotonically increase or decrease, but it rather fluctuates depending on the train speed and on the position of the node with respect to the passing train.

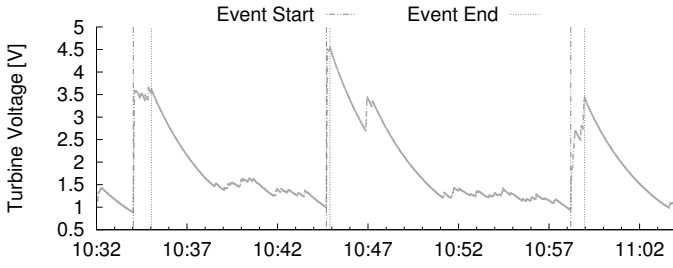


Fig. 9. Detection of train passage events performed by node number 6. Dashed lines mark the time interval in which the event has occurred.

TABLE I. STATISTICS ABOUT TRAIN PASSAGE EVENTS DETECTED DURING THE PERIOD 14 – 18 MAY: NUMBER OF TRAINS DETECTED BY EACH NODE, MEAN INTER-ARRIVAL TIME (MIT) AND STANDARD DEVIATION BETWEEN THE PASSAGE OF TWO CONSECUTIVE TRAINS AT DAYTIME; AVERAGE DURATION AND STANDARD DEVIATION OF EACH HARVESTING EVENT.

Node	Detected trains	MIT (m:s)	σ (m:s)	Duration (s)	σ (s)
1	143	11:58	06:13	20	19.84
2	141	12:47	06:00	26	21.30
3	141	12:47	06:00	24	24.26
4	143	12:49	06:13	25	16.76
5	142	12:50	05:56	27	13.85
6	142	13:04	06:09	29	16.34

corresponding voltage at maximum power point (as explained in sec. III-A). Fig. 10 shows the voltage conversion performed for node number 6.

During train passage events, the capacitor voltage measured by the nodes alternates between increasing and decreasing periods (an example is shown in Fig. 9). When the voltage increases, the harvested power is calculated according to a look-up table which relates voltages at MPP and actual power values. When the capacitor voltage decreases, however, the actual power that is being harvested by the node can not be known exactly. To estimate the actual voltage of the micro-turbine during such decreasing periods we defined three different heuristics:

- **Best:** the power harvested is computed by considering the voltage measured at the end of the last increasing period;
- **Worst:** the harvested power is assumed to be zero;
- **Average:** the power harvested is computed by considering a value equal to half of the voltage measured at the end of the last increasing period.

Fig. 11 shows an example of application of such heuristics. The Worst heuristic is the most pessimistic one, as it assumes the voltage of the micro-turbine during voltage decreasing periods to be zero. The Best heuristic, instead, assumes that during decreasing periods the voltage of the micro-turbine remains constant, thus leading to the most optimistic estimation of the harvested power. Finally, the Average heuristic is a balance between the other two.

Another possible approach to estimate the voltage of the micro-turbine during capacitor voltage dropping periods is to use interpolation techniques to approximate the decreasing trend. However, the duration of such events is usually quite limited (4 – 10 seconds or 2 – 5 voltage samples), making it

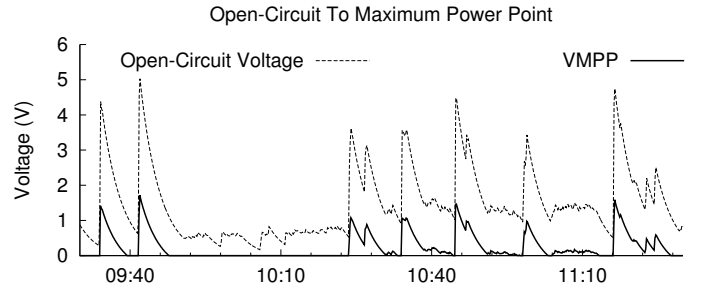


Fig. 10. Open-circuit voltage to V_{MPP} conversion performed according to the empirical Equation (1). Plot refers to the data collected by node number 6.

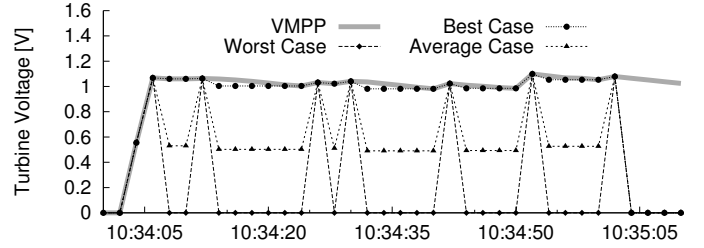


Fig. 11. Turbine voltage estimation during voltage dropping periods using the Worst, Best and Average heuristics.

difficult to obtain good results by interpolating the empirical data. For this reason, the heuristic-based technique is the estimation method that best suits the data collected from the nodes deployed in the underground tunnel.

V. POWER MANAGEMENT ALGORITHM

This section deals with the power management algorithms to determine how to choose the proper rectifier bridge so as to maximize the power harvested by the node with minimal overhead.

A. Adaptive strategy

The first and simplest power management strategy considered is the one called *adaptive*. Such strategy constantly keeps track of the power generated by the micro-turbine over time and dynamically selects the rectifier to be used such as to maximize the efficiency of the conversion to be performed. More in details, the *adaptive* strategy uses the passive-Schottky topology when the harvested power is lower than $2mW$ and the active topology when the harvested power is equal to or greater than such threshold (Fig. 4). The *adaptive* strategy potentially achieves the best results in terms of harvested energy, assuming that it can sample the incoming power with a high frequency to detect all the relevant events. In such case, it always selects the most efficient rectifier bridge to use. However, it also suffers from the highest overhead among the possible power management strategies, as it needs to constantly monitor the power generated by the turbine.

To reduce such overhead in practical settings, the power generated by the micro-turbine is sampled every f seconds. Every time that a sample is collected, the rectifier topology

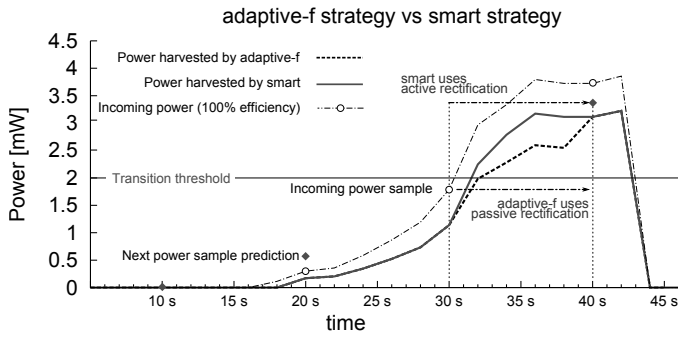


Fig. 12. Example of application of the adaptive- f and of the smart strategies during a wind energy harvesting event.

to use is dynamically selected by comparing the sampled value with the transition threshold of $2mW$ discussed in Section III-B. Once selected, such topology is then used for the successive time-slot of f seconds, i.e., until a new sample is collected. Based on the sampling period, this reduces the overhead of the system, at the cost of potentially not selecting the most efficient rectifier bridge at any given time t . For brevity, we indicate with *adaptive- f* the *adaptive* strategy performing a power sample every f seconds.

B. Smart strategy

In this section, a third strategy, called *smart*, is proposed, which aims at improving the selection of the best rectifier topology based on the current harvesting conditions.

The *smart* strategy is similar to the *adaptive- f* approach, as it samples the power generated by the micro-turbine every f seconds. However, differently from the *adaptive- f* strategy, the *smart* strategy does not select the most efficient rectifier bridge solely comparing the current power sample with the threshold of $2mW$. Rather, it tries to estimate the potential power intake during the next f seconds and selects the rectifier topology that maximizes the conversion efficiency of such *expected* power.

The predicted power intake during the current time-slot is estimated by means of regression analysis, a statistical technique widely employed for prediction. In particular, a simple linear regression is implemented, in which the prediction variable is the time, denoted by variable t , and the response variable is the estimated power at time t , denoted by p^t . Given the set of the last n power observations, $\{(t_{i-n}, p_{i-n}^t), \dots, (t_i, p_i^t)\}$, the goal of simple linear regression is to find the equation of the straight line which would provide the best fit for the observed data points. Such equation can be found by minimizing the sum of squared residuals of the linear regression [42]. The *smart* strategy performs a simple linear regression over a sliding window whose size is set so as to match the average duration of the wind harvesting events detected by the nodes in the tunnel (Table I). The number n of observations over which the regression is performed thus depends on the sampling period f .

Figure 12 shows an example of application of the *adaptive- f* and of the *smart* strategies during a wind energy harvesting event detected by node 2. The dashed line with white circle

dots represent the amount of incoming power at the ideal conversion efficiency of 100%. In such example, the linear regression is performed over a sliding window of 30 seconds and the sampling period is set to 10 seconds. At time $t = 30$ seconds, the incoming power sampled by node 2 is below the transition threshold of $2mW$. Thus, the *adaptive- f* strategy selects the passive rectifier as the topology to be used for the current time-slot. However, since a train is approaching and the incoming power is rapidly rising, this leads to a reduced conversion efficiency during the successive 10 seconds. The *smart* strategy, instead, by performing linear regression over the last 3 power samples, predicts that the expected power during the current time-slot is going to exceed the transition threshold. It thus successfully selects the active rectification topology, resulting in a higher amount of energy being harvested during the successive 10 seconds. At time $t = 40$ seconds, the incoming power sampled by node 2 is above the transition threshold of $2mW$, so both strategies select the active rectifier as the topology to be used for that time-slot.

In addition to power forecasting, the *smart* strategy also implements two specific optimizations for the tunnel scenario. In fact, being such scenario almost totally predictable, knowledge of the environment may be exploited to further reduce the overhead of the system and avoid unnecessary sampling. The *smart* strategy leverages the train detection algorithm detailed in Section IV-B to determine when sampling should be performed. In particular, whenever a train passage is detected, no sampling is performed for the successive six minutes, which is the minimum expected inter-arrival time between two consecutive train passages (Table I). Moreover, the *smart* strategy does not perform sampling at night time, as no trains passed in the tunnel during the train test phase between 8 : 10 PM and 8 : 15 AM.

VI. EXPERIMENTAL COMPARISON OF POWER MANAGEMENT POLICIES

This section discusses the results of the performance evaluation of the power management techniques described in Section V, as well as the passive-Schottky and active topologies detailed in Section III-B. For each rectification strategy, the metrics considered in each evaluation are: 1) average energy harvested per day by each node, and 2) overhead of the system, in terms of the average number of sampling performed per day by a node using a given strategy.

Fig. 13 shows the average energy gathered per day by each node in the tunnel scenario, based on the rectification technique used by the nodes. Energy is computed as follows: the voltage measurement recorded by the node is converted to the voltage at maximum power point according to equation (1). To estimate the actual voltage of the micro-turbine during capacitor voltage dropping periods, the Best, Worst and Average heuristics described in Section IV-C are used. Once the micro-turbine voltage has been estimated the power harvested by the node is computed according to a look-up table which relates voltages at MPP and actual power values. The final value of the harvested power is then computed by taking into account the efficiency of the rectification strategy used

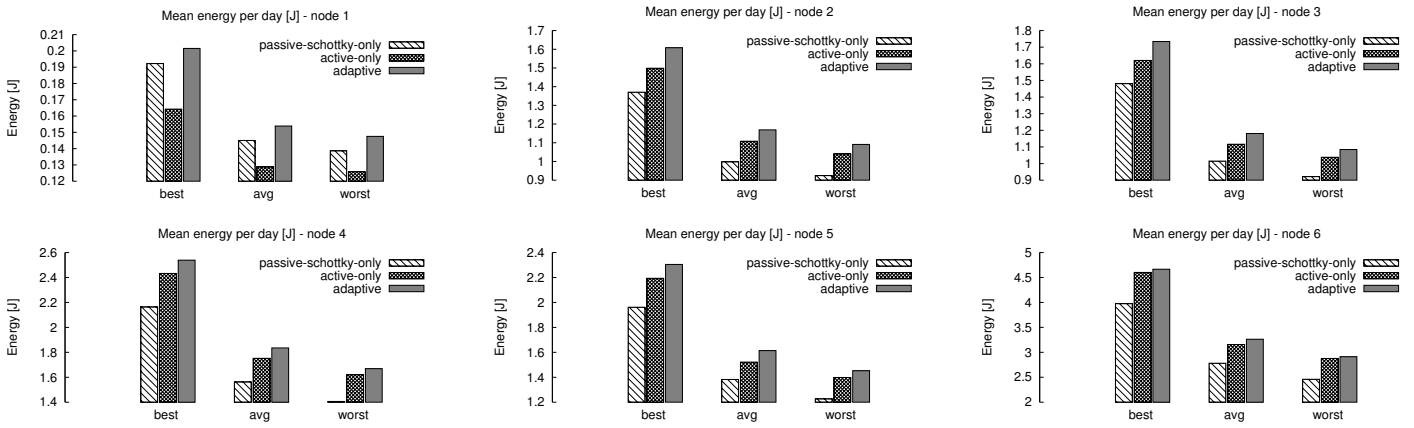


Fig. 13. Comparison of the average amount of energy harvested per day by each node, when using the passive-Schottky, active or adaptive rectification techniques.

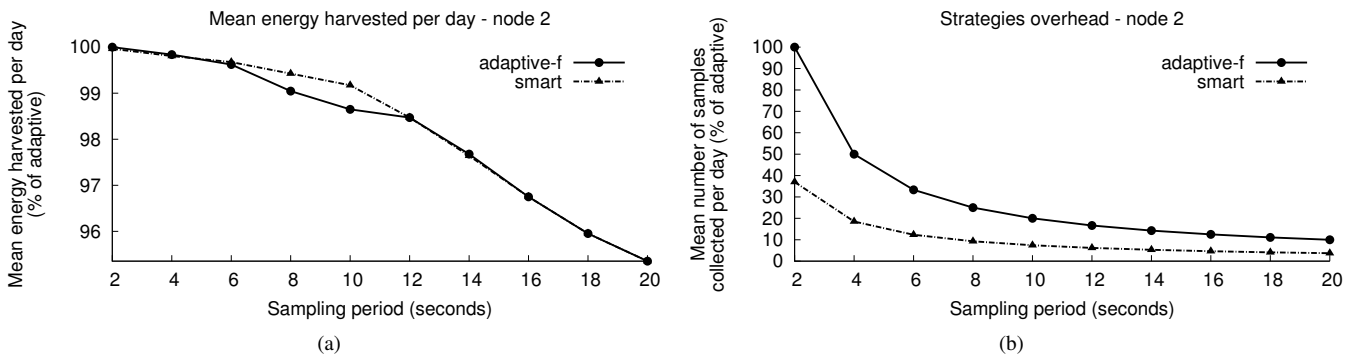


Fig. 14. Comparison between *smart* and *adaptive-f* strategies for varying sampling periods: (a) average energy harvested per day, as a percentage of the energy harvested by the *adaptive* strategy, and (b) strategies overhead in terms of average number of samples collected per day, as a percentage of the overhead introduced by the *adaptive* strategy.

(Fig. 4). In this estimation process the power consumption of the control circuitry of the only-active and adaptive rectifiers is implicitly considered as it has been involved in the SPICE characterization of each topology performed in section III-B. Moreover, the efficiency of the regulation stage discussed in section III-C is considered. In other words, the overall efficiency of the adopted architecture starts from 50% when the input power is lower than the transition threshold and rises up over 72% when the incoming power exceeds the threshold.

Results are plotted for the *adaptive* rectification techniques and for the passive-Schottky and active topologies. As can be seen from Fig. 13, the energy harvested per day varies significantly for different nodes, depending on their position in the tunnel. In particular, node 1, being deployed very close to the train station, harvests significantly less energy than the other nodes. For all the nodes, the *adaptive* technique consistently outperforms the passive-Schottky-only and active-only topologies, resulting in significant increment of the total energy harvested per day. More in detail, the average energy harvested per day by using the adaptive strategy is, depending on the considered node, up to 18% higher than that harvested by the passive-Schottky-only topology, and up to 22% higher than that harvested by the active-only topology. Such improvements are

achieved when the wind flow intensity is frequently varying and the average output power from the turbine is very close to the transition threshold depicted in Fig. 4. In such conditions, the adaptive rectification technique significantly outperforms the others, achieving the highest rectification efficiency for any wind speed. If the wind flow intensity is predominantly either high or low, instead, the performance of adaptive rectification is much closer to that of the active-only or passive-Schottky-only topology, as the hybrid rectifier consistently operates in only one of the two configurations. For example, since node 6 mostly operates under high wind speed conditions, the improvement of the hybrid solution with respect to the active-only rectifier is less than 3.4% (Fig. 13). Overall, when considering all the nodes operating under different wind speed conditions, the average increase in harvested energy obtained by the adaptive strategy is of 15% with respect to the passive-Schottky-only topology, and of 7% with respect to the active-only topology.

As mentioned before, the *adaptive* strategy always achieves the best results in terms of harvested energy, but it suffers from the highest overhead. Our second set of experiments shows the trade-off between the energy harvested by the nodes and the overhead introduced by managing the adaptive

rectifier. The performance of the *adaptive-f* and of the *smart* strategies are thoroughly studied in terms of harvested energy and system overhead, for varying sampling periods. In this set of experiments, the window size of the linear regression performed by the *smart* strategy is set to 30 seconds.

Fig. 14(a) shows the average energy harvested per day by both the *adaptive-f* and the *smart* strategies, as a percentage of the energy harvested by the *adaptive* strategy, which represents indeed an upper bound on the energy harvestable by using the topologies described in Section III. Fig. 14(b) shows the overhead introduced by the *adaptive-f* and *smart* strategies, in terms of the average number of sampling performed per day, as a percentage of the overhead introduced by the *adaptive* strategy. Due to space constraints, results are reported only for node 2, but they show similar trends for different nodes.

As it can be seen in Fig. 14(b), the *smart* strategy significantly reduces the overhead with respect to the *adaptive-f* approach, without impairing the capability of the nodes to harvest energy from air-flows. In fact, the number of sampling performed by the *smart* strategy is almost one third of that performed by *adaptive-f*. At the same time, the average energy per day collected by the *smart* strategy is always greater or equal to that of the *adaptive-f* strategy (Fig. 14(a)). For instance, by performing a sampling every 10s the *smart* strategy is able to harvest an amount of energy per day that is more than 99% of that harvested by the *adaptive* strategy, introducing an overhead that is only $\approx 7\%$ of that of the *adaptive* strategy. When using the same setting for the sampling period (i.e., one sample every 10 seconds), the *adaptive-f* strategy harvests slightly less energy than the *smart* strategy, but its overhead is almost three times greater than that introduced by the *smart* strategy. The greatest improvement in terms of average energy harvested per day is obtained by the *smart* strategy for sampling periods of 8 – 10 seconds. Being the window size set to 30 seconds, this corresponds to performing the linear regression over the last 3 power observations. Finally, the passive-Schottky-only and active-only topologies do not introduce any additional overhead, but they harvest only 93% and 85% of the energy obtained by the *adaptive* strategy.

The additional amount of energy delivered by the adaptive rectifier leads to a significant extension of the nodes' lifetime. In fact, considering negligible the power consumption during the sleep time, each node consumes about 12mJ during its activity time, namely data sensing and wireless transmission. Therefore, an increment of 400mJ as shown in Fig. 13 means about 33 more sample and transmission activities.

VII. CONCLUSIONS

In this paper a power management technique for improving the efficiency of harvesting energy from air-flows generated by trains passing in an underground tunnel is presented. The key feature of the proposed solution is the adaptive AC-DC converter, a hybrid voltage rectifier which exploits both passive and active topologies combined with power prediction algorithms. In fact, the rectifiers reported in literature are designed to maximize the efficiency with very low input voltage and power, where it is crucial to avoid power wasting in the *microwatts*. We have demonstrated, when the input power varies

in a wider range (i.e. from *microwatts* to *tens of milliwatts*), that a hybrid solution can achieve performance comparable to the on-chip rectifiers. In particular, our combined approach significantly outperforms other rectification topologies, resulting in an increase of efficiency between 10% and 30% with respect to the only-passive and the only-active rectifiers. Furthermore it is a cost effective and simple design, suitable for environmental sources which produce up to milliwatts, as the air-flow energy harvesting. To evaluate the effectiveness of the presented approach, a data collection campaign has been conducted in a tunnel of the new Underground *Metro B1* line in Rome. Six Telos B motes equipped with wind micro-turbines are used to instruments 220m of tunnel with the aim to collect air-flow data for 33 days. It is found that by using the adaptive AC-DC converter nodes deployed in the tunnel can harvest up to 22% more energy than that harvested by using the active-only or the passive-only topology. Finally, a *smart* power-management strategy which exploits the predictable tunnel scenario has been proposed to significantly reduce the overhead of the system. Such strategy performs an average number of sampling per day that is only 7% of that of the *adaptive* strategy and almost one third of that of the *adaptive-f* strategy. At the same time, the average energy per day collected by the *smart* strategy is always greater or equal of that of the *adaptive-f* strategy.

REFERENCES

- [1] S. Basagni, M. Y. Naderi, C. Petrioli, and D. Spenza, "Wireless Sensor Networks with Energy Harvesting," in *Mobile Ad Hoc Networking: Cutting Edge Directions*, ser. IEEE Series on Digital and Mobile Communication. Hoboken, NJ: John Wiley and Sons, Inc., March 2013, ch. 20.
- [2] S. Sudevalayam and P. Kulkarni, "Energy harvesting sensor nodes: survey and implications," *IEEE Communications Surveys Tutorials*, vol. 13, no. 3, pp. 443–461, Third quarter 2011.
- [3] A. S. Weddell, M. Magno, G. V. Merrett, D. Brunelli, B. M. Al-Hashimi, and L. Benini, "A survey of multi-source energy harvesting systems," in *Proceedings of the Conference on Design, Automation and Test in Europe*, ser. DATE '13. San Jose, CA, USA: EDA Consortium, 2013, pp. 905–908. [Online]. Available: <http://dl.acm.org/citation.cfm?id=2485288.2485505>
- [4] G.K. Ottman, H.F. Hofmann, A.C. Bhatt, and G.A. Lesieutre, "Adaptive piezoelectric energy harvesting circuit for wireless remote power supply," *IEEE Transactions on Power Electronics*, vol. 17, no. 5, pp. 669 – 676, Sep 2002.
- [5] D. Porcarelli, D. Balsamo, D. Brunelli, and G. Paci, "Perpetual and low-cost power meter for monitoring residential and industrial appliances," in *Proceedings of the Conference on Design, Automation and Test in Europe*, ser. DATE '13. San Jose, CA, USA: EDA Consortium, 2013, pp. 1155–1160. [Online]. Available: <http://dl.acm.org/citation.cfm?id=2485288.2485567>
- [6] H. Lhermet, C. Condemine, M. Plissonnier, R. Salot, P. Audebert, and M. Rosset, "Efficient power management circuit: from thermal energy harvesting to above-ic microbattery energy storage," *IEEE Journal of Solid-State Circuits*, vol. 43, no. 1, pp. 246 –255, Jan 2008.
- [7] F.I. Simjee and P.H. Chou, "Efficient charging of supercapacitors for extended lifetime of wireless sensor nodes," *IEEE Transactions on Power Electronics*, vol. 23, no. 3, pp. 1526 –1536, May 2008.
- [8] M. Magno, S. Marinkovic, D. Brunelli, E. Popovici, B. O'Flynn, and L. Benini, "Smart power unit with ultra low power radio trigger capabilities for wireless sensor networks," in *Design, Automation Test in Europe Conference Exhibition (DATE), 2012*, 2012, pp. 75–80.

- [9] J.W. Kimball, B.T. Kuhn and R.S. Balog, "A system design approach for unattended solar energy harvesting supply," *IEEE Transactions on Power Electronics*, vol. 24, no. 4, pp. 952–962, Apr 2009.
- [10] D. Porcarelli, D. Brunelli, M. Magno, and L. Benini, "A multi-harvester architecture with hybrid storage devices and smart capabilities for low power systems," in *Power Electronics, Electrical Drives, Automation and Motion (SPEEDAM), 2012 International Symposium on*, June 2012, pp. 946–951.
- [11] Y. K. Tan and S. Panda, "Optimized wind energy harvesting system using resistance emulator and active rectifier for wireless sensor node," *IEEE Transactions on Power Electronics*, vol. 26, no. 1, pp. 38–50, Jan 2011.
- [12] D. Carli, D. Brunelli, D. Bertozzi and L. Benini, "A high-efficiency wind-flow energy harvester using micro turbine," in *Power Electronics Electrical Drives Automation and Motion (SPEEDAM), 2010 International Symposium*, Jun 14-16 2010, pp. 778–783.
- [13] M. A. Weimer, T. S. Paing, and R. A. Zane, "Remote area wind energy harvesting for low-power autonomous sensors," in *Proc. 37th IEEE Power Electronics*, Jun 18-22 2006, pp. 1–5.
- [14] A. Cammarano, D. Spenza, and C. Petrioli, "Energy-harvesting WSNs for structural health monitoring of underground train tunnels," in *Proceedings of the 32nd IEEE International Conference on Computer Communications, IEEE INFOCOM 2013 WKSHPs*, Torino, Italy, April 14-19 2013, pp. 75–76.
- [15] U. M. Colesanti, A. Lo Russo, M. Paoli, C. Petrioli, and A. Vitaletti, "Structural Health Monitoring in an Underground Construction Site: The Roman Experience," in *Proceedings of the 11th ACM Conference on Embedded Networked Sensor Systems*, ser. SenSys '13. New York, NY, USA: ACM, 2013, pp. 46:1–46:2. [Online]. Available: <http://doi.acm.org/10.1145/2517351.2517420>
- [16] M. Ceriotti, M. Corra, L. D'Orazio, R. Doriguzzi, D. Facchin, S. Guna, G. Jesi, R. Cigno, L. Mottola, A. Murphy, M. Pescalli, G. Picco, D. Pregolato, and C. Torghelle, "Is there light at the ends of the tunnel? Wireless sensor networks for adaptive lighting in road tunnels," in *Proc. of the 10th International Conference on Information Processing in Sensor Networks*, ser. IPSN 2011, april 2011, pp. 187–198.
- [17] L. Mottola, G. P. Picco, M. Ceriotti, c. Gunà, and A. L. Murphy, "Not all wireless sensor networks are created equal: A comparative study on tunnels," *ACM Trans. Sen. Netw.*, vol. 7, no. 2, pp. 15:1–15:33, Sep. 2010.
- [18] F. Stajano, N. Hoult, I. Wassell, P. Bennett, C. Middleton, and K. Soga, "Smart bridges, smart tunnels: Transforming wireless sensor networks from research prototypes into robust engineering infrastructure," *Ad Hoc Networks*, vol. 8, no. 8, pp. 872 – 888, 2010.
- [19] S. Cheekiralla, "Wireless sensor network-based tunnel monitoring," Stockholm, Sweden, June 20-21 2005, poster presentation.
- [20] R. Liu, I. Wassell, and K. Soga, "Relay node placement for Wireless Sensor Networks deployed in tunnels," in *Proc. of IEEE 6th International Conference on Wireless and Mobile Computing, Networking and Communications (WiMob)*, oct. 2010, pp. 144–150.
- [21] D. Wu, L. Bao, and R. Li, "A holistic approach to wireless sensor network routing in underground tunnel environments," *Comput. Commun.*, vol. 33, no. 13, pp. 1566–1573, Aug. 2010.
- [22] J. Lu, S. Liu, Q. Wu, and Q. Qiu, "Accurate modeling and prediction of energy availability in energy harvesting real-time embedded systems," in *The First International Green Computing Conference*, aug 15-18 2010, pp. 469–476.
- [23] C. Moser, D. Brunelli, L. Thiele, and L. Benini, "Real-time scheduling with regenerative energy," in *Real-Time Systems, 2006. 18th Euromicro Conference on*, 2006, pp. 10 pp.–270.
- [24] A. Cammarano, C. Petrioli, and D. Spenza, "Improving Energy Predictions in EH-WSNs with Pro-Energy-VLT," in *Proceedings of the 11th ACM Conference on Embedded Networked Sensor Systems*, ser. SenSys '13. New York, NY, USA: ACM, 2013, pp. 41:1–41:2. [Online]. Available: <http://doi.acm.org/10.1145/2517351.2517413>
- [25] D. K. Noh and K. Kang, "Balanced energy allocation scheme for a solar-powered sensor system and its effects on network-wide performance," *Journal of Computer and System Sciences*, vol. 77 (5), pp. 917–932, September 2011.
- [26] A. Cammarano, C. Petrioli, and D. Spenza, "Pro-Energy: a novel energy prediction model for solar and wind energy harvesting WSNs," in *Proceeding of the 9th IEEE International Conference on Mobile Ad hoc and Sensor Systems*, ser. IEEE MASS 2012, Las Vegas, Nevada, USA, 8-11 October 2012, pp. 75–83.
- [27] N. Sharma, J. Gummeson, D. Irwin, and P. Shenoy, "Cloudy Computing: Leveraging Weather Forecasts in Energy Harvesting Sensor Systems," in *Proceedings of the 7th Annual IEEE Communications Society Conference on Sensor, Mesh and Ad Hoc Communications and Networks*, ser. IEEE SECON 2010, Boston, Massachusetts, USA, June 21-25, 2010, pp. 1–9.
- [28] J. Piorno, C. Bergonzini, D. Atienza, and T. Rosing, "Prediction and management in energy harvested wireless sensor nodes," in *Proc. of Wireless VITAE 2009*, Aalborg, Denmark, May 17-20, 2009, pp. 6–10.
- [29] A. Kansal, J. Hsu, S. Zahedi, and M. B. Srivastava, "Power management in energy harvesting sensor networks," *ACM Trans. Embed. Comput. Syst.*, vol. 6, no. 4, September 2007.
- [30] C. Bergonzini, D. Brunelli, and L. Benini, "Algorithms for harvested energy prediction in batteryless wireless sensor networks," in *Advances in sensors and Interfaces, 2009. IWASI 2009. 3rd International Workshop on*, June 2009, pp. 144–149.
- [31] F. Blaabjerg and K. Ma, "Future on power electronics for wind turbine systems," *Emerging and Selected Topics in Power Electronics, IEEE Journal of*, vol. 1, no. 3, pp. 139–152, Sept 2013.
- [32] G. Mandic, A. Nasiri, E. Ghotbi, and E. Muljadi, "Lithium-ion capacitor energy storage integrated with variable speed wind turbines for power smoothing," *Emerging and Selected Topics in Power Electronics, IEEE Journal of*, vol. 1, no. 4, pp. 287–295, Dec 2013.
- [33] T. S. Paing, and R. A. Zane, "Resistor emulation approach to low-power energy harvesting," in *Proc. 37th IEEE Power Electronics Specialists Conference (PESC 06)*, Jun 18-22 2006, pp. 1–7.
- [34] M. Magno, D. Boyle, D. Brunelli, B. O'Flynn, E. Popovici, and L. Benini, "Extended wireless monitoring through intelligent hybrid energy supply," *Industrial Electronics, IEEE Transactions on*, vol. 61, no. 4, pp. 1871–1881, April 2014.
- [35] L. Karthikeyan, B. Amrutur, "Signal-powered low-drop-diode equivalent circuit for full-wave bridge rectifier," *IEEE Transactions on Power Electronics*, vol. 27, no. 10, pp. 4192 – 4201, Oct 2012.
- [36] Y.-H. Lam, W.-H. Ki, C.-Y. Tsui, "Integrated low-loss cmos active rectifier for wirelessly powered devices," *IEEE Transactions on Circuits and Systems II: Express Briefs*, vol. 53, no. 12, pp. 1378–1382, Dec 2006.
- [37] E. Dallago, D. Miatton, G. Venchi, V. Bottarel, G. Frattini, G. Ricotti, M. Schipani, "Active autonomous ac-dc converter for piezoelectric energy scavenging systems," in *IEEE Custom Integrated Circuits Conference, 2008 (CICC 2008)*, Sept 2008, pp. 555 – 558.
- [38] S. Cheng, Y. Jin, Y. Rao, D.P. Arnold, "An active voltage doubling ac/dc converter for low-voltage energy harvesting applications," *IEEE Transactions on Power Electronics*, vol. 26, no. 8, pp. 2258–2265, Aug 2011.
- [39] S. Cheng, R. Sathe, R.D. Natarajan, D.P. Arnold, "A voltage-multiplying self-powered ac/dc converter with 0.35-v minimum input voltage for energy harvesting applications," *IEEE Transactions on Power Electronics*, vol. 26, no. 9, pp. 2542–2549, Sept 2011.
- [40] Crossbow Technology, "TelosB mote platform datasheet," 2004, document Part Number: 6020-0094-01 Rev B.
- [41] TinyOS, "The TinyOS operating system for embedded wireless devices," <http://www.tinyos.net/>. Last accessed Dec 5, 2102.
- [42] N. Ye, *The handbook of data mining*. Lawrence Erlbaum, 2003.



Danilo Porcarelli is a Research Fellow at the Energy-efficient Embedded Systems group, University of Bologna, where he received his Master degree in electronic engineering. The most important themes of his research are on power management techniques and extension of the lifetime of wireless sensor networks (WSN). In this field has worked actively both on the energy efficiency of the nodes and the network and on the design of harvesters, such as solar and air-flow scavengers, and using the hydrogen fuel cells to feed the nodes and to recharge the

batteries. He has collaborated with several universities and IT companies such as Telecom Italia, Italy.



Alessandro Cammarano received the laurea degree with the highest honors in Computer Science in 2010 from the University of Rome La Sapienza. He is currently a third year PhD student at the Computer Science Department of the same University, and member of the SENSES laboratory. His research interests focus on wireless sensor networks design, cognitive radio networks, energy harvesting wireless sensor networks and energy prediction models.



Dora Spenza is a Postdoc researcher at the Department of Computer Science of University of Rome "La Sapienza", and member of the SENSES (Sensor network and embedded systems) laboratory. She holds a B.S. (2006, cum laude), a M.S. (2009, cum laude) and a PhD (2013) in Computer Science from University of Rome "La Sapienza". From March to July 2011, she was a visiting scholar at the Computer Science and Engineering Department at Penn State University, USA. Her research interests concern green wireless networking, with an emphasis

on energy-harvesting wireless sensor networks, resource allocation and tasking for environmental and structural monitoring. Dora Spenza is the recipient of the 2010 Google European Doctoral Fellowship in Wireless Networking.



Chiara Petrioli (SM'06) received the Ph.D. in Computer Engineering from Rome University "La Sapienza," Italy, in 1998. She is currently a full professor at University of Rome La Sapienza Computer Science Department, where she leads the Sensor Networks and Embedded Systems laboratory (SENSES lab). She also leads the Cyber Physical System lab of "La Sapienza" center for Cyber Intelligence and Information Security, and is a founding partner of "La Sapienza" spinoff WSENSE S.r.l. Her research interests focus on the design and optimization of wireless, embedded and cyber physical systems. On these topics Prof. Petrioli has published over a hundred papers in prominent international journals and conferences. Prof. Petrioli is member of the steering committee of ACM SenSys, workshop co-chair of ACM MobiCom 2014, general chair of ACM WUWNET 2014, general chair of ACM SenSys 2013. She has been member of the steering committee and associate editor of IEEE Transactions on Mobile Computing, associate editor of IEEE Transactions on Vehicular Technology, member of the executive committee of ACM SIGMOBILE, and has been program co-chair of leading conferences in the field such as ACM MobiCom and IEEE SECON. Prof. Petrioli was a Fulbright scholar.



Davide Brunelli (M'10) is Assistant Professor at University of Trento since 2010. He holds a M.S. (2002, cum laude) and a PhD in Electrical Engineering (2007) from the University of Bologna. From 2005 to 2007 he has been visiting researcher at ETHZ studying to develop methodologies for Energy Harvesting aware embedded design. He was scientific supervisor of several EU FP7 projects and he was leading industrial cooperation activities with Telecom Italia. His research interests concern Smart Grids and the development of new techniques of energy

scavenging for wireless sensor networks (WSNs) and embedded systems, the optimization of low-power and low-cost WSNs, and the interaction and design issues in embedded personal and wearable devices.



Luca Benini is Full Professor at the University of Bologna and he is the chair of digital Circuits and systems at ETHZ. He has served as Chief Architect for the Platform2012/STHORM project in STmicroelectronics, Grenoble in the period 2009-2013. He has held visiting and consulting researcher positions at EPFL, IMEC, Hewlett-Packard Laboratories, Stanford University. Dr. Benini's research interests are in energy-efficient system design and Multi-Core SoC design. He is also active in the area of energy-efficient smart sensors and sensor networks

for biomedical and ambient intelligence applications. He has published more than 700 papers in peer-reviewed international journals and conferences, four books and several book chapters. He is a Fellow of the IEEE and a member of the Academia Europaea.